



Supplement of

Archaeal community composition in Holocene methane pockmarks of the Gdańsk Basin (Baltic Sea, Poland): insights from tetraether lipids and 16S rRNA analysis

Izabela De Mey-Śnieżyńska et al.

Correspondence to: Izabela De Mey-Śnieżyńska (i.sniezynska@uw.edu.pl)

The copyright of individual parts of the supplement might differ from the article licence.

Table S1. Characterisation of the core sampling stations (P – methane pockmark site; S – reference sites).

Station (polygon) ID	Coordinates	Water depth and morphology	Gas emission to the water column	Porewater freshening ¹	Activity status
P/MET1-MP		Water depth of ~80 m, relative depth of ~2 m, surface area of ~1200 × 500 m, with spatially variable morphology (Brodecka et al., 2013).	Spatially heterogeneous gas seepage (Majewski and Klusek, 2011; Brodecka et al., 2013); periodic release of single gas bubbles and low-intensity, scattered gas ebullition to the water column, weaker and less focused than at MET1-BH (Kurowski et al., 2024; Łukawska-Matuszewska et al., 2025).	Porewater freshening/upward infiltration of freshened groundwater, indicated by Cl ⁻ profiles in this study and by previous MET1-MP porewater evidence (Idczak et al., 2020; Brodecka-Goluch et al., 2022)	Active pockmark with observed gas seepage and porewater freshening.
S/MET1-MP	MET1 area 54°34'N, 19°10'E	Water depth of ~78 m; flat seabed, 100-150 m from the edge of P/MET1-MP pockmark.	No gas emissions to the water column observed; gas/methane present in the sediment.	Very weak porewater freshening, based on Cl ⁻ profiles in this study.	Reference site.
P/MET1-BH		Water depth of 88 m, relative depth of ~10 m, diameter of ~50 m; a conical depression with an internal cascade structure (Brodecka-Goluch et al., 2020; Idczak et al., 2020).	Constant, intensive gas flares from the pockmark interior, with plumes rising up to ~20 m into the water column (Idczak et al., 2020; Łukawska-Matuszewska et al., 2025).	Periodic porewater and near-bottom water freshening/upward infiltration of freshwater, indicated by Cl ⁻ profiles in this study and by previous SGD evidence (Idczak et al., 2020; Brodecka-Goluch et al., 2022).	Active pockmark with strong gas ebullition/flares and porewater freshening.
S/MET1-BH		Water depth of 79 m; flat seabed with no distinct morphological features, 100-150 m from the edge of the P/MET1-BH pockmark.	No gas emissions into the water column observed; gas/methane present in the sediments.	Very weak porewater freshening, based on Cl ⁻ profiles in this study.	Reference site.
P/MET3	MET3 area 54°44'N, 19°11'E	Water depth of 97 m, relative depth of ~2 m, and surface area of ~100 × 75 m; cloud-like shape	Occasional release of single gas bubbles was reported in previous observations; no gas ebullition was observed in the echogram used in this study (Fig. S1).	No porewater freshening except at the bottom of the sampled interval; no clear evidence of active freshened porewater discharge	Inactive pockmark during the present observations; weak/occasional gas seepage

¹ Porewater freshening indicated by Cl⁻ profiles in this study is interpreted as evidence of relative porewater freshening with respect to the reference core, and of the influence of freshened porewater, with the indication that the absence of chloride depletion does not exclude recirculated submarine groundwater discharge.

		(Brodecka-Goluch et al., 2020).		in the sampled core or in previous research campaigns (Brodecka-Goluch et al., 2020).	reported previously.
S/MET3		Water depth of 95 m; flat seabed with no distinct morphological features, 100-150 m from the edge of the P/MET3 pockmark.	No gas emissions into the water column observed; gas/methane present in the sediment.	No porewater freshening was observed, based on Cl ⁻ profiles in this study.	Reference site.
P/MET4	MET4 area 55°07' N 19°00' E	Water depth of 104 m, relative depth of ~5 m, and surface area of ~150 × 100 m (Brodecka-Goluch et al., 2020).	Gas seepage registered by split-beam echosounder (Fig. S1).	Slight porewater freshening, based on Cl ⁻ profiles in this study, but weak/uncertain evidence for active freshwater seepage during previous research campaigns (Brodecka-Goluch et al., 2020).	Weakly active pockmark with observed gas seepage and weak porewater freshening.
S/MET4		Water depth of 99 m; flat seabed with no distinct morphological features, 100-150 m from the edge of the P/MET4 pockmark.	No gas emissions into the water column observed; gas/methane present in the sediment.	No porewater freshening was observed, based on Cl ⁻ profiles in this study.	Reference site.

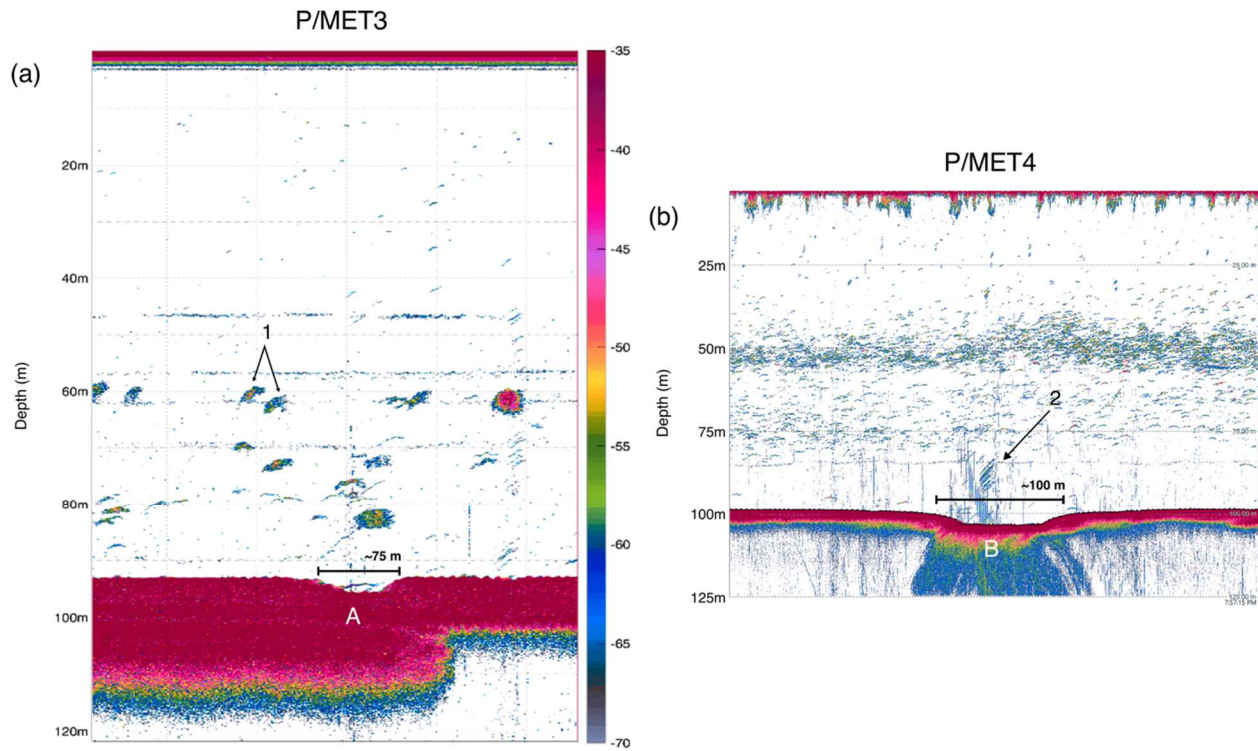


Fig. S1. Echograms of two pockmarks recorded by a Simrad EK80 split-beam echosounder, Gdańsk Deep, Gdańsk Basin. (a) P/MET3, a pockmark depression (A) with an approximate diameter of ~75 m and shoals of fish in the overlying water column (1); no gas seepage is observed. (b) P/MET4, a pockmark depression (B) with an approximate diameter of ~100 m and gas release above the pockmark (2).

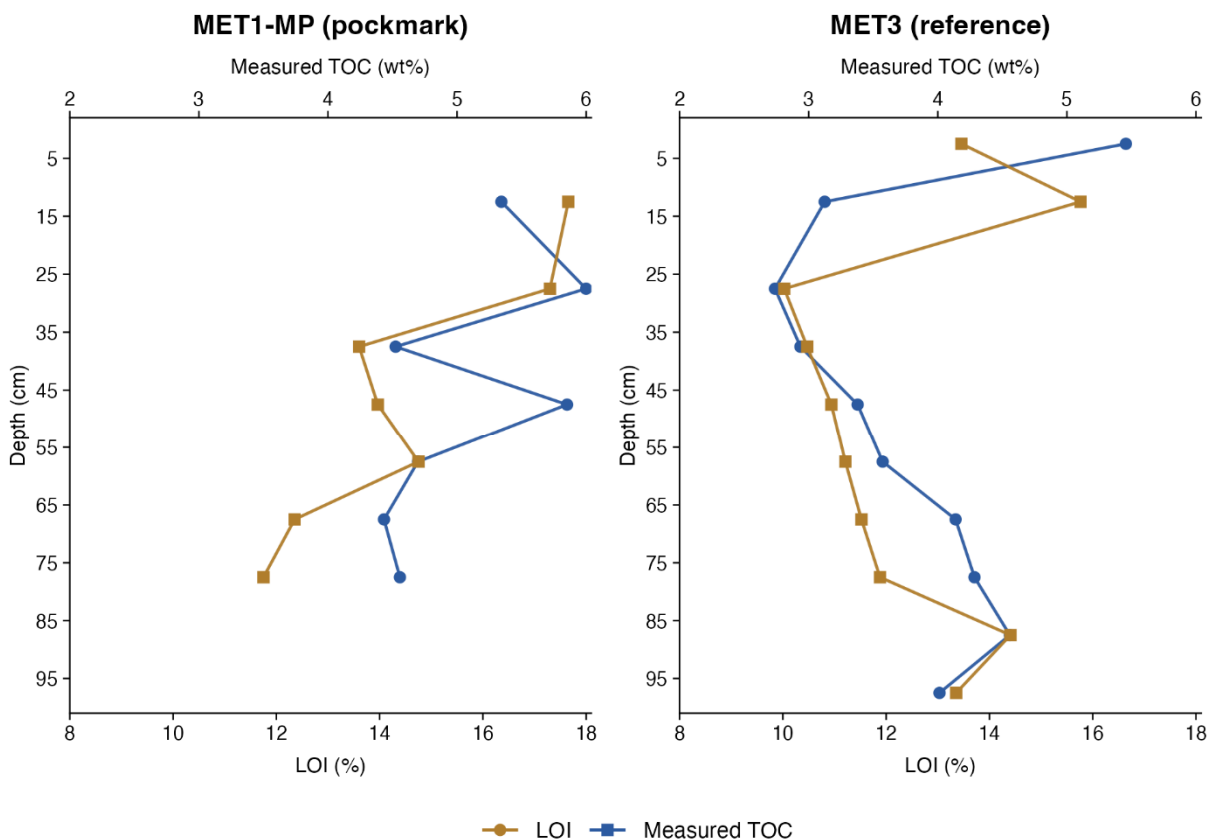


Fig. S2. Comparison of loss-on-ignition values (LOI%) and directly measured total organic carbon (TOC wt%) in two representative sediment cores from the south-eastern Baltic Sea: the MET1-MP pockmark core from the Gulf of Gdańsk and the MET3 reference core from the Gdańsk Deep. Both parameters are plotted against sediment depth (cm bsf). This comparison was used to assess whether LOI captures the main stratigraphic variability in organic matter content. Across both cores, LOI and measured TOC show a positive correlation ($n = 17$, $R^2 = 0.43$, $p = 0.004$), supporting the use of LOI as a qualitative, trend-level proxy for variability in bulk organic matter. Although sample-scale offsets occur between LOI and TOC, the profiles broadly reproduce comparable downcore patterns.

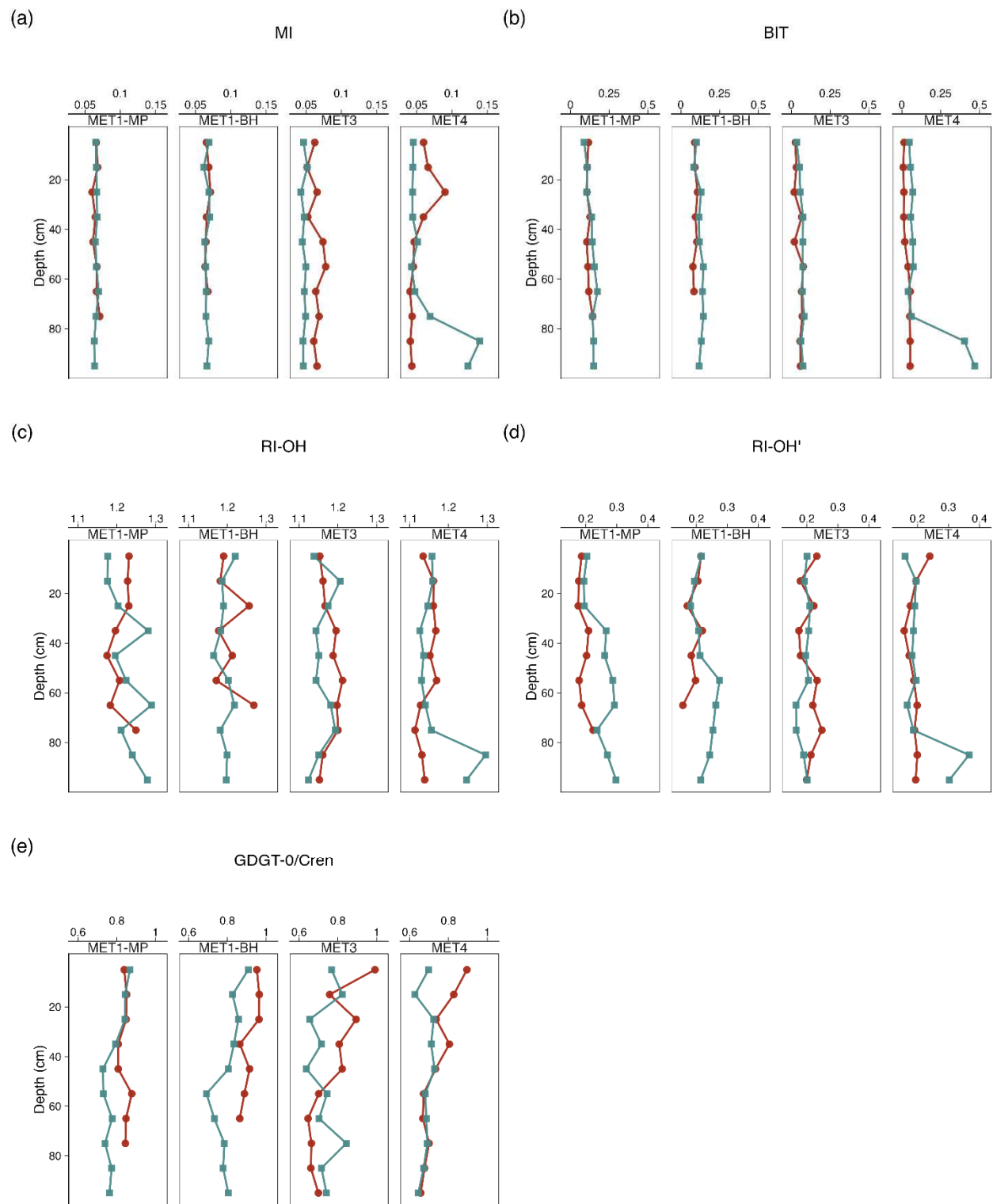


Fig. S3. Downcore variability of (a) Methane Index (MI), (b) Branched and Isoprenoid Tetraether index (BIT), (c-d) hydroxylated GDGT ring indices (RI-OH, RI-OH'), and (e) GDGT-0/cren ratio, showing differences in absolute values between pockmark and non-pockmark cores. MI and GDGT-0/cren values

are consistently low and show no AOM imprint on the iGDGT pool. BIT index shows a marine organic matter source. RI-OH and RI-OH' values are within the norm for Baltic Sea surface sediments.

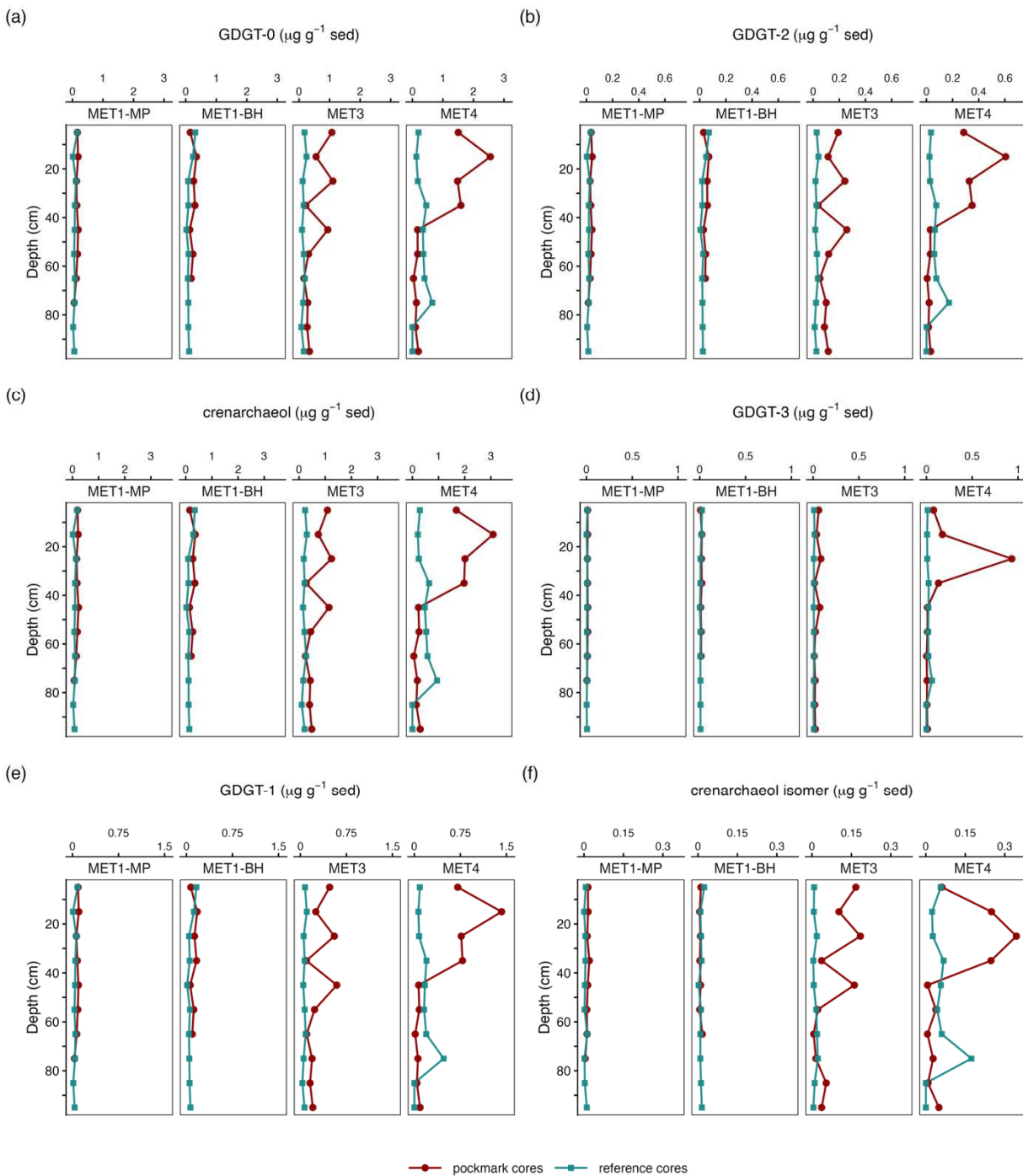


Fig. S4. Downcore variation of archaeal lipid biomarkers (a–f): iGDGTs (GDGT-0–3, cren, cren') in sediment cores from the Gulf of Gdańsk (MET1-MP, MET1-BH) and the Gdańsk Deep (MET3, MET4), south-eastern Baltic Sea. Concentrations ($\mu\text{g g}^{-1}$ sediment) are plotted against depth below sea floor (cm bsf). In all cores, GDGT-0 and crenarchaeol dominate the iGDGT pool, whereas GDGT-1–3 and cren' occur at lower concentrations. Pockmark sediment cores generally exhibit elevated biomarker

concentrations relative to reference sediment cores, with the strongest enrichments observed in the Gdańsk Deep cores.

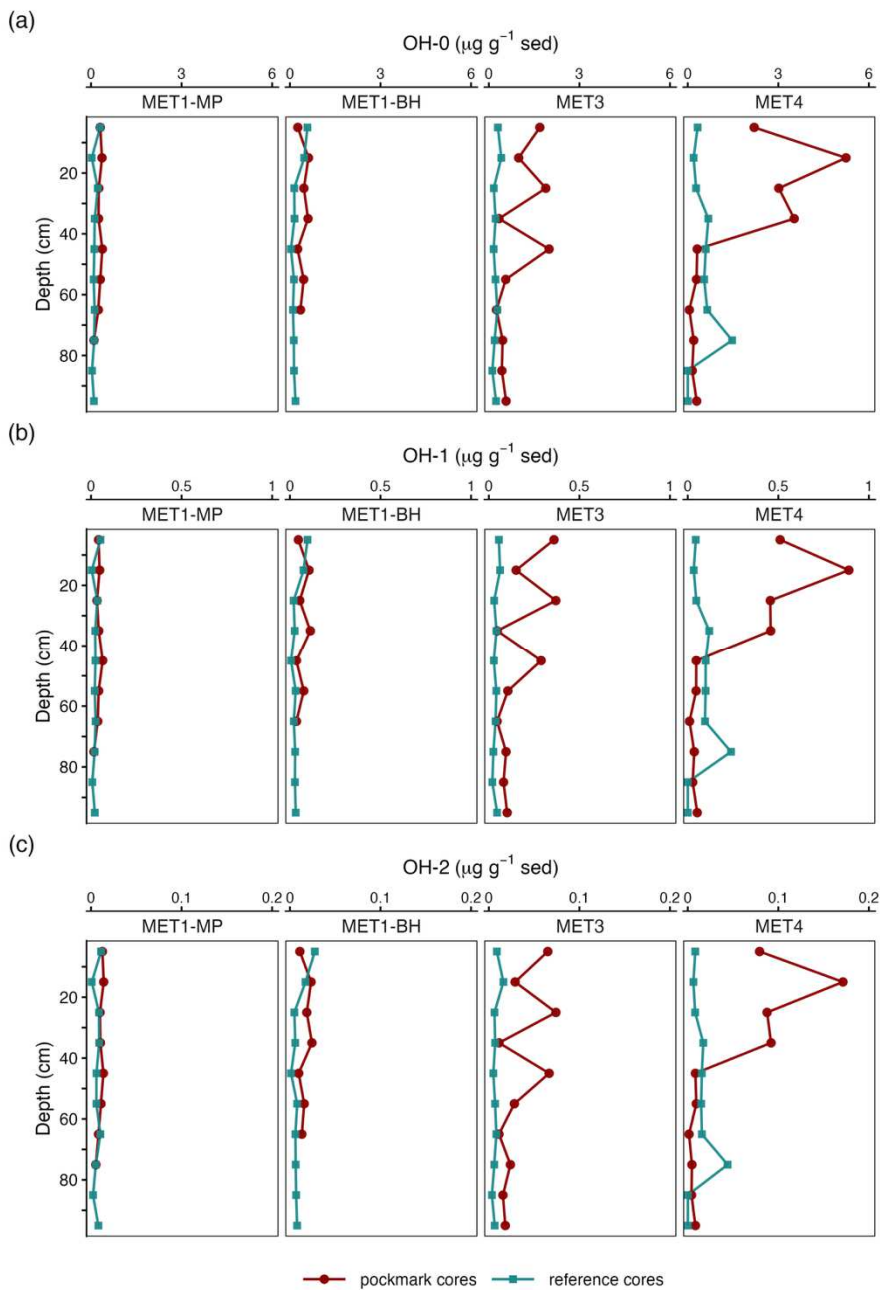


Fig. S5. Downcore variations in archaeal lipid biomarkers (OH-GDGT-0–2; $\mu\text{g g}^{-1}$ sediment) in sediment cores from the Gulf of Gdańsk (MET1-MP, MET1-BH) and the Gdańsk Deep (MET3, MET4), south-eastern Baltic Sea. Concentrations ($\mu\text{g g}^{-1}$ sediment) are plotted against depth bsf (cm). OH-GDGT-0 is the predominant compound, with lower contributions from OH-GDGT-1 and OH-GDGT-2. The profiles show distinct downcore variability, with generally higher concentrations in pockmark sediments.

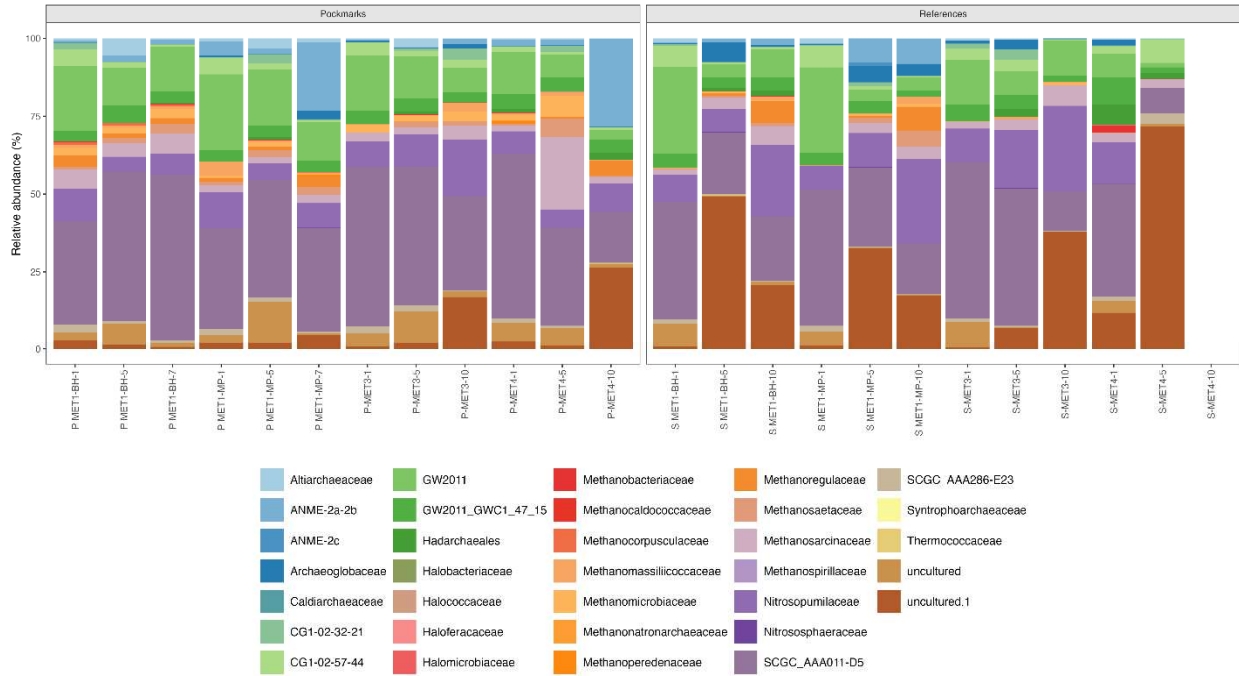
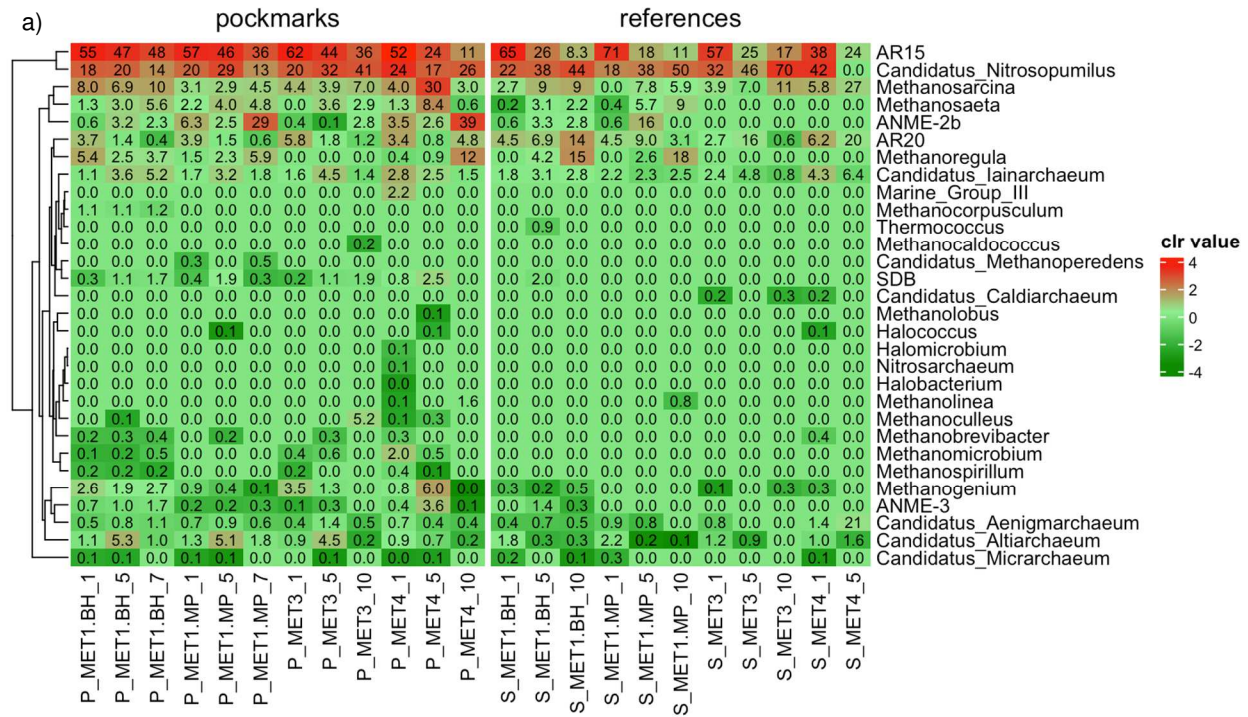


Fig. S6. Extended family-level relative abundance profiles of archaeal communities in pockmark and reference sediment cores. Stacked bar plots show the relative abundance (%) of archaeal families in each sample, grouped by site type (pockmarks and references) and by depth interval within each study location (MET1-BH, MET1-MP, MET3, MET4). Only families with relative abundances above a defined threshold (five reads) are shown.



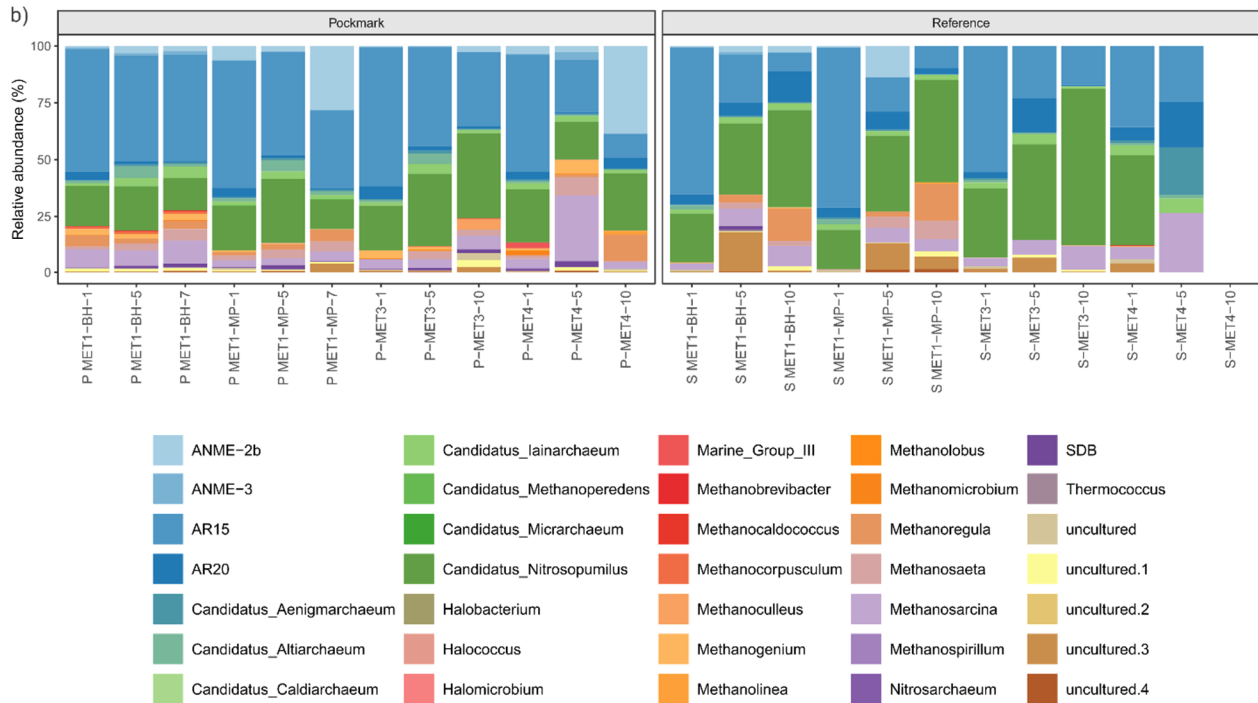


Fig. S7. (a) Heatmap of archaeal genus-level distributions across pockmark and reference sediment cores. Rows represent archaeal genera (and selected uncultured lineages), and columns represent individual samples grouped by site type (pockmarks and references) and by depth horizon at the study locations (MET1-BH, MET1-MP, MET3, MET4). Colour intensity reflects centred log-ratio (CLR)-transformed relative abundances (%) in samples, with red indicating higher and green indicating lower relative enrichment. Hierarchical clustering of genera (left dendrogram) highlights patterns of co-occurrence and differential distribution between environments. (b) Genus-level composition of archaeal communities in pockmark and reference sediment cores. Stacked bar plots show the relative abundance (%) of archaeal genera in each sample, grouped by site type (pockmarks and references) and by depth interval within each study location (MET1-BH, MET1-MP, MET3, MET4). Only genera exceeding a defined threshold (five reads) are shown.

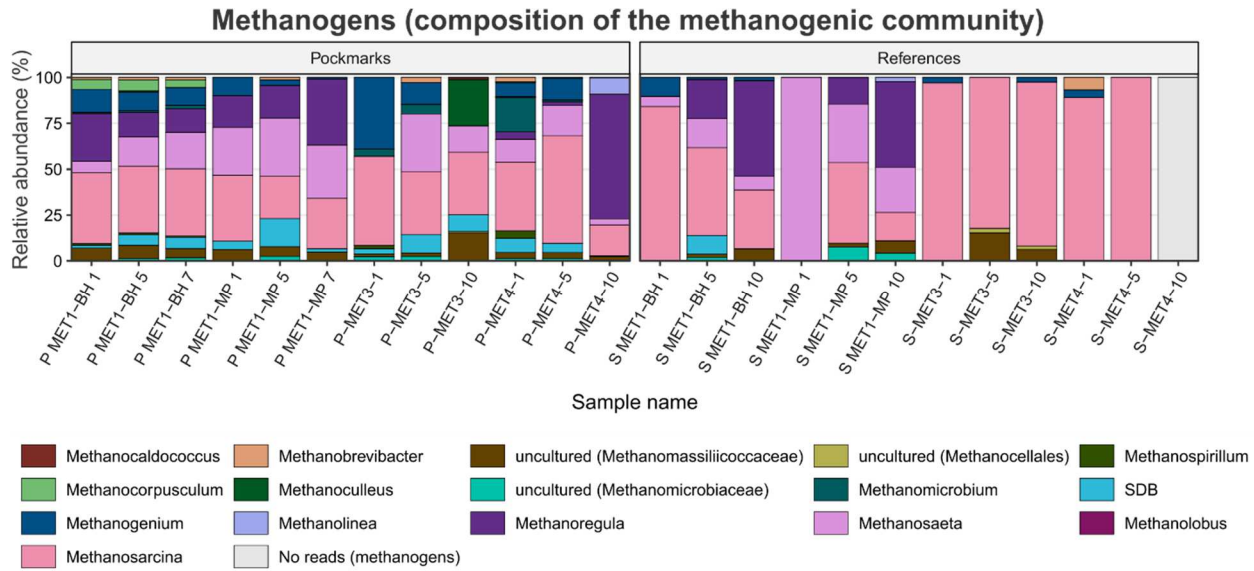


Fig. S8. Relative abundance of methanogenic archaea at the genus level in pockmark and reference sediment cores. Bars show the proportional contribution of methanogenic taxa to each sample's methanogenic community. Colours correspond to the genera shown in the legend; uncultured lineages are annotated at their lowest resolved rank (family or order). Grey bars indicate samples with no methanogen reads detected.

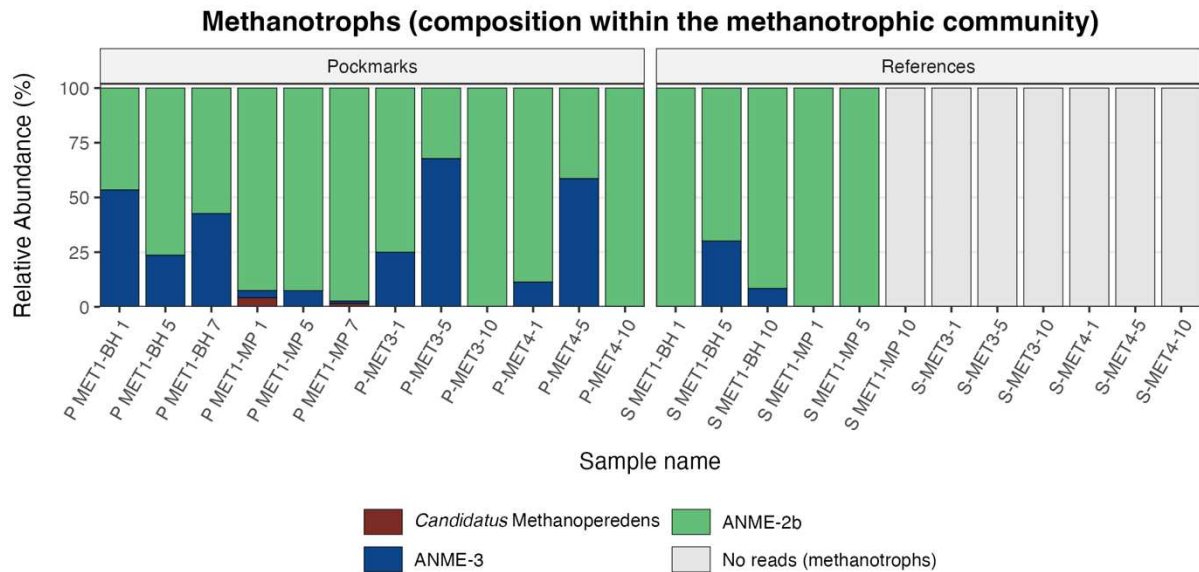


Fig. S9. Relative abundance of methanotrophic archaeal groups in pockmark and reference sediment cores at the genus level. Bars show the proportional contribution of methanotroph taxa within each sample's methanotroph community. Colours indicate ANME-2b, ANME-3, and *Candidatus* Methanoperedens; grey bars denote samples with no detected methanotroph reads.

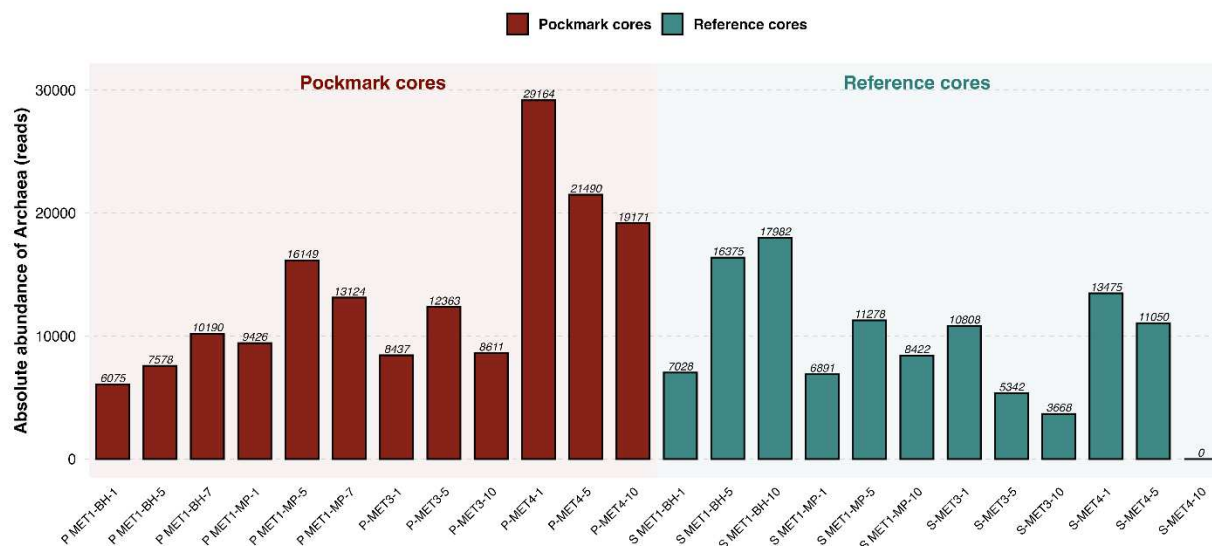


Fig. S10. Absolute abundance of archaea (reads at the class level) in pockmark and reference sediments at distinct depth horizons (surface denoted as 1; mid-depth as 5; bottom as 7 and 10).

References

- Brodecka, A., Majewski, P., Bolałek, J., Klusek, Z., 2013. Geochemical and acoustic evidence for the occurrence of methane in sediments of the Polish sector of the southern Baltic Sea*. *Oceanologia* 55, 951–978. <https://doi.org/10.5697/oc.55-4.951>
- Brodecka-Goluch, A., Idczak, J., Gorska, N., Bolałek, J., 2020. Geophysical and geochemical characteristics of four different pockmark sites located in the Gdańsk Basin, in: *Earth System Changes and Baltic Sea Coasts*. Jastarnia, pp. 89–90.
- Brodecka-Goluch, A., Łukawska-Matuszewska, K., Kotarba, M.J., Borkowski, A., Idczak, J., Bolałek, J., 2022. Biogeochemistry of three different shallow gas systems in continental shelf sediments of the South-Eastern Baltic Sea (Gulf of Gdańsk): Carbon cycling, origin of methane and microbial community composition. *Chemical Geology* 597, 120799. <https://doi.org/10.1016/j.chemgeo.2022.120799>
- Idczak, J., Brodecka-Goluch, A., Łukawska-Matuszewska, K., Graca, B., Gorska, N., Klusek, Z., Pezacki, P.D., Bolałek, J., 2020. A geophysical, geochemical and microbiological study of a newly discovered pockmark with active gas seepage and submarine groundwater discharge (MET1-BH, central Gulf of Gdańsk, southern Baltic Sea). *Science of The Total Environment* 742, 140306. <https://doi.org/10.1016/j.scitotenv.2020.140306>
- Kurowski, S., Łukawska-Matuszewska, K., Čović, A., Jozić, D., Brodecka-Goluch, A., 2024. Effects of pockmark activity on iron cycling and mineral composition in continental shelf sediments (southern Baltic Sea). *Biogeochemistry* 167, 135–154. <https://doi.org/10.1007/s10533-024-01127-1>

- Łukawska-Matuszewska, K., Brodecka-Goluch, A., Czachor, A., Rios-Quintero, R., 2025. Gas bubble release areas as new potential hot spots for water column enrichment with nutrients in eutrophicated sea. *Marine Environmental Research* 205, 106981. <https://doi.org/10.1016/j.marenvres.2025.106981>
- Majewski, P., Klusek, Z., 2011. Expressions of shallow gas in the Gdansk Basin. *Zeszyty Naukowe Akademii Marynarki Wojennej* 52, 61–71.